SCIENCE CHINA
Technological Sciences

February 2013 Vol.56 No.2: 492–498
doi: 10.1007/s11431-012-5078-0

Effect of seed electron injection on chorus-driven acceleration of radiation belt electrons

YAN Qi[1,2], SHI LiQing[1*] & LIU SiQing[1]

[1] *Center for Space Science and Applied Research, Chinese Academy of Sciences, Beijing 100190, China;*
[2] *Graduate University of Chinese Academy of Sciences, Beijing 100049, China*

Received May 25, 2012; accepted October 22, 2012; published online November 9, 2012

Using the hybrid finite difference method, we solve the Fokker-Planck equation to study the effect of seed electron injection on acceleration of radiation belt electrons driven by chorus waves. Numerical results show that in the absence of injection chorus waves can accelerate electrons at large pitch angles (α_e>60°), producing enhancements in the phase space density (PSD) of (1–2 MeV) electrons by a factor of 100–1000 within 1–2 days. In the presence of injection, chorus waves yield increase in PSD of electrons by accelerating the injected seed electrons. Meanwhile, the PSD evolution increases as the pitch angle increases but decreases as electron energy increases. Moreover, the PSD evolution can extend to higher energies with a time scale of 1–2 days for 1–2 MeV energies. When the injection increases by a factor of 10 higher than the initial value and remains for about two days, maximum values of PSD for 1 or 2 MeV increase to 6 or 3 times respectively higher than those without injection in two days. The current results suggest that the injected seed electrons play an important role in the evolution of the radiation belt electrons.

seed electrons, chorus waves, radiation belt electrons

Citation: Yan Q, Shi L Q, Liu S Q. Effect of seed electron injection on chorus-driven acceleration of radiation belt electrons. Sci China Tech Sci, 2013, 56: 492–498, doi: 10.1007/s11431-012-5078-0

1 Introduction

The radiation belts which contain energetic (100 keV to a few MeV) electrons are separated into an inner region and an outer region by the slot of a lower electron flux [1]. The outer radiation belt is highly variable particularly during geomagnetic storms or other disturbances and energetic electron flux can vary by several orders of magnitude over periods from hours to days [2–6]. This variation of energetic electrons causes serious risk to spacecraft and astronauts. Therefore, it is important to study the distribution and evolution of outer radiation belt electrons.

Numerous possible mechanisms have been proposed to explain the dramatic variation of the energetic electron flux in the outer radiation belt. During geomagnetic storms, dramatic variation of the geomagnetic field occurs primarily due to growth and decay of the ring current. In response to such a large scale variation of geomagnetic storms in time and space, radiation belt electrons experience an adiabatic transport [6–11]. In this process, three adiabatic invariants keep constant, whereas variations in the pitch angle, energy and *L*-shell occur. However, previous observations have shown that the energetic electron flux does not return to the previous storm level [12], indicating that besides the adiabatic process some non-adiabatic transport processes also contribute to the flux variation. One of those processes is radial diffusion driven by the ultra-low-frequency (ULF) waves, e.g., the inward radial diffusion is able to accelerate electrons because of strengthening of the magnetic field and

*Corresponding author (email: slq@earth.sepc.ac.cn)

the conservation of the first adiabatic invariant [13–15]. Another adiabatic process is resonant interaction between electrons and various electromagnetic waves with different frequencies [16–27]. This process can produce either stochastic acceleration or precipitation loss of energetic electrons in the inner magnetosphere, leading to the variation in flux of energetic electrons during storms.

Observational work [28–31] has demonstrated that chorus emissions are often present in the low-density region outside the plasmapause, with typical frequencies between 0.05 and 0.8 $|\Omega_e|$ ($|\Omega_e|$ is the electron gyrofrequency) over the magnetic local time 2200–1300. The typical amplitudes for chorus waves are about 1–100 pT and can reach 1 nT during strong storms, even 100 mV m^{-1} in some extreme cases. Previous studies [17, 25] have shown that radiation belt electrons can be efficiently accelerated by the resonant interaction between electrons and chorus waves.

Seed (tens to hundreds of keV) electrons, which transport towards the earth from the magnetotail during substorms, are an important source of energetic electrons in the radiation belt [32–34]. In order for this, seed electrons need to be accelerated to high energies by some mechanisms. Apart from the adiabatic process of acceleration, the resonant interaction with chorus waves may also play an important role. However, there are currently few studies on the influence of seed electron injection on the evolution of the radiation belt electrons. In this study, we shall provide a quantitative simulation in the framework of the quasi-linear theory.

2 Numerical method

Here, we use the quasi-linear model developed by Su et al. [35] to simulate the interaction between electrons and chorus waves propagating along the magnetic field. We then solve the 2D bounce-averaged Fokker-Planck equation by using the hybrid finite difference (HFD) method developed by Xiao et al. [25]. Such HFD method, which is efficient and stable for treating whistler-electron interaction, has been adopted and proved very well by numerous groups [6, 25–27, 35–45].

The quasi-linear bounce-averaged Fokker-Planck diffusion equation describing resonant interaction between electrons and chorus waves can be written as [46]

$$\frac{\partial f}{\partial t}=\frac{1}{G}\frac{\partial}{\partial \alpha_e}\left[G\left(\langle D_{\alpha\alpha}\rangle\frac{\partial f}{\partial \alpha_e}+\langle D_{\alpha p}\rangle\frac{\partial f}{\partial p}\right)\right]+\frac{1}{G}\frac{\partial}{\partial p}\left[G\left(\langle D_{p\alpha}\rangle\frac{\partial f}{\partial \alpha_e}+\langle D_{pp}\rangle\frac{\partial f}{\partial p}\right)\right], \tag{1}$$

$$G=p^2T(\alpha_e)\sin\alpha_e\cos\alpha_e, \tag{2}$$

$$T\approx 1.30-0.56\sin\alpha_e, \tag{3}$$

where f denotes the phase space density (PSD) of electrons, t denotes time, α_e and p represent equatorial pitch angle and momentum of electrons, $\langle D_{\alpha\alpha}\rangle$, $\langle D_{pp}\rangle$, $\langle D_{\alpha p}\rangle=\langle D_{p\alpha}\rangle$ stand for bounce-averaged pitch-angle, momentum and cross diffusion coefficients respectively.

Assuming that the background magnetic field is a dipole field, we can obtain expressions of bounce-averaged diffusion coefficients above as follows [47]:

$$\langle D_{\alpha\alpha}\rangle=\frac{1}{T}\int_0^{\lambda_m}D_{\alpha\alpha}\frac{\cos\alpha}{\cos^2\alpha_e}\cos^7\lambda\,\mathrm{d}\lambda, \tag{4}$$

$$\langle D_{pp}\rangle=\frac{1}{T}\int_0^{\lambda_m}D_{pp}\frac{\left(1+3\sin^2\lambda\right)^{1/2}}{\cos\alpha}\cos\lambda\,\mathrm{d}\lambda, \tag{5}$$

$$\langle D_{\alpha p}\rangle=\frac{1}{T}\int_0^{\lambda_m}D_{\alpha p}\frac{\left(1+3\sin^2\lambda\right)^{1/4}}{\cos\alpha_e}\cos^4\lambda\,\mathrm{d}\lambda, \tag{6}$$

where λ is magnetic latitude, λ_m is the latitude of the mirror point determined by α_e, α is the local pitch angle at λ (corresponding to α_e in the equatorial plane), $D_{\alpha\alpha}$, D_{pp}, $D_{\alpha p}$= $D_{p\alpha}$ which represent the local pitch angle, momentum and cross diffusion coefficients, are given by [48, 49]

$$D_{\alpha\alpha}=\frac{|\Omega_e|^2}{p^2}\left(\frac{p^2}{\gamma^2}I_0-2\cos\alpha\frac{cp}{\gamma}I_1+\cos^2\alpha c^2I_2\right), \tag{7}$$

$$D_{pp}=c^2|\Omega_e|^2\sin^2\alpha I_2, \tag{8}$$

$$D_{\alpha p}=-c|\Omega_e|^2\sin\alpha\left(\frac{I_1}{\gamma}-\frac{c\cos\alpha}{p}I_2\right), \tag{9}$$

$$I_n=\pi\sum_{\omega_r}\left\{\frac{B_\omega^2}{B_0^2(\lambda)}\left(\frac{\omega_r}{ck_r}\right)^n\left|1-\cos\alpha\frac{p}{\gamma}\frac{\mathrm{d}k}{\mathrm{d}\omega}\right|_{\omega=\omega_r}^{-1}\right\}, \tag{10}$$

$$B_0(\lambda)=3.12\times10^4\frac{\left(1+3\sin^2\lambda\right)^{1/2}}{L^3\cos^6\lambda}\mathrm{nT}, \tag{11}$$

$$B_\omega^2=\begin{cases}B_n\exp\left[-(\omega-\omega_m)^2/\delta\omega^2\right], & \omega_l\leqslant\omega\leqslant\omega_2\\ 0, \quad \text{otherwise,}\end{cases} \tag{12}$$

$$B_n=\frac{2B_t^2}{\pi^{1/2}\delta\omega}\left[\mathrm{erf}\left(\frac{\omega_2-\omega_m}{\delta\omega}\right)+\mathrm{erf}\left(\frac{\omega_m-\omega_l}{\delta\omega}\right)\right]^{-1}, \tag{13}$$

where, ω_r and k_r which are the resonant wave frequency and wave number, satisfy both the resonant condition between electrons and the field-aligned chorus waves

$$\omega-(v\cos\alpha)k=|\Omega_e|/\gamma, \tag{14}$$

and the dispersion of the chorus waves

$$c^2k^2 = \omega^2 - \frac{\omega\omega_{pe}^2}{\omega - |\Omega_e|}. \quad (15)$$

Here n = 0, 1, 2, ω_{pe} is plasma frequency, c is the speed of light, v is the velocity of electrons, $\gamma = \left(1 - v^2/c^2\right)^{-1}$ is Lorentz factor, and B_0 denotes the ambient magnetic field. We assume that chorus waves follow a Gaussian frequency distribution. erf(x) is the error function, B_ω^2 is the wave spectral intensity, B_t is the wave magnitude, B_n is the normalized factor, ω_m is the center frequency, $\delta\omega$ is the half width, ω_1 and ω_2 are the lower and upper frequencies.

We evaluate the effect of wave-particle scattering at L = 4.5. We choose the simulating area as [0°, 90°]×[0.2 MeV, 5.0 MeV] in the space (α_e, E_k). The numerical grid is 101×101 and the time step is 5 s. We assume the initial PSD as a typical kappa distribution [50]:

$$f\left(t=0, \alpha_e, p\right) = C\left(\frac{p\sin\alpha_e}{\theta_\kappa}\right)^{2l}\left[1+\frac{p^2}{\kappa\theta_\kappa^2}\right]^{-(\kappa+l+1)}, \quad (16)$$

$$C = \frac{N\Gamma\left(\kappa+l+1\right)}{\pi^{3/2}\theta_\kappa^3\kappa^{l+3/2}\Gamma\left(l+1\right)\Gamma\left(\kappa-1/2\right)}. \quad (17)$$

Here l is the loss cone index, θ_κ^2 is the effective thermal parameter, N is the number density, κ is the spectral index, and Γ is the gamma function. In our simulation, we choose κ=6, $\theta_\kappa^2 = 0.15$, l=0.5 based on the observations.

Assume a rapid precipitation of electrons into the atmosphere inside the loss-cone $\alpha_e=\alpha_L$ ($\sin\alpha_L=L^{-3/2}(4-3/L)^{-1/4}$). We take $f(\alpha_e=\alpha_L)=0$ and $\partial f(\alpha_e=\pi/2)/\partial\alpha_e = 0$. The upper energy boundary condition is f=0 at E_k= 5 MeV, implying no net loss or increase of electrons at high energies.

To study the effect of the seed electron injection, we choose the injection boundary model with 200 keV seed electrons as $f(E_k$=0.2 MeV)=$C_t f(t$=0, E_k=0.2 MeV), where C_t is a function of time. We simulate the evolution of PSD in two cases (Figure 1): (A), C_t=1, corresponding to the lower fixed boundary condition; (B), variation of C_t with time, corresponding to electron injection increasing to ten times of the initial value in the first one hour and lasting for about two days.

3 Results and discussion

Since chorus wave covers a broad MLT region, we consider the dayside and nightside chorus waves for the evaluation of diffusion terms. The parameters of chorus waves on both sides are chosen as follows: on the dayside, ω_1=0.1$|\Omega_{eq}|$ ($|\Omega_{eq}|$ is the equatorial electron gyrofrequency), ω_2=0.3$|\Omega_{eq}|$, $\delta\omega$=0.1$|\Omega_{eq}|$, ω_m=0.2$|\Omega_{eq}|$, $B_t=10^{0.75+0.04\lambda}$[pT] (here $\lambda\leqslant35°$) and the equatorial $\omega_{pe}/|\Omega_e|$ is 4.6; on nightside, ω_1=0.05$|\Omega_{eq}|$, ω_2=0.65$|\Omega_{eq}|$, $\delta\omega$=0.15$|\Omega_{eq}|$, ω_m=0.35$|\Omega_{eq}|$, B_t=50 [pT] (here $\lambda\leqslant15°$) and the equatorial $\omega_{pe}/|\Omega_e|$ 3.8. Those parameters are also used by other studies [21, 22, 25, 28]. Since the drift orbit of electrons on the dayside and nightside are about 25% of the whole drift orbit, in the following we apply 25% drift averaging for both the dayside and nightside.

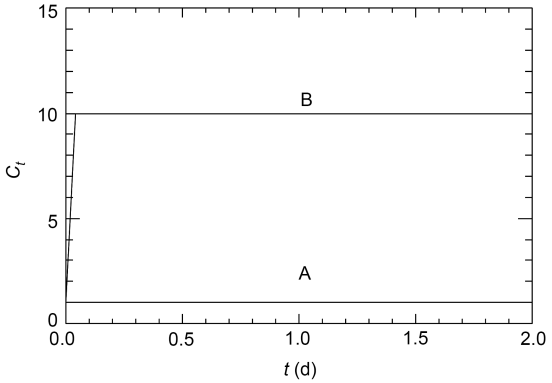

Figure 1 Lower energy boundary conditions of cases A and B.

Figure 2 plots two-dimensional bounce-averaged pitch angle, momentum and cross diffusion coefficients. It is shown that diffusion coefficients basically increase as the pitch angle increases when α_e>60°, but vary slowly and smoothly when α_e<40°. Diffusion coefficients in the region of α_e>60° and E_k<1.0 MeV are generally one order larger than those coefficients outside this region.

Figure 3 shows the temporal PSD evolution from a numerical solution to the diffusion equation (1) by using the HFD method. The left and right panels are the results of case A and case B, respectively. In case A (without injection), electron PSD with energy above 1.0 MeV has a remarkable increase in larger pitch angle area (α_e>60°). In case B (with injection), the injected seed electrons can be efficiently accelerated to very high energies by chorus waves, producing an increase in PSD of radiation belt electrons. In particular, PSD for α_e>60° and E_k<0.5 MeV increases more rapidly, corresponding to distribution features of diffusion coefficients that they generally increase as the pitch angle increases if α_e>60°.

Figure 4 presents the PSD variation of electrons with the kinetic energy at the fixed pitch angles 20° and 70° for cases A and B. At α_e=70°, in the absence of injection, PSD gradually increases with time, with an higher enhancement for the higher energies below 2.0 MeV. For 2.0 MeV, PSD can reach three orders of magnitude higher than the initial one, suggesting that chorus waves can efficiently accelerate radiation belt electrons and enhance electron PSD by 2–3 orders of magnitude. At α_e=20°, electron PSD increases a little below 1.0 MeV but drops a little above 1.0 MeV in both cases A and B, indicating that chorus waves have a

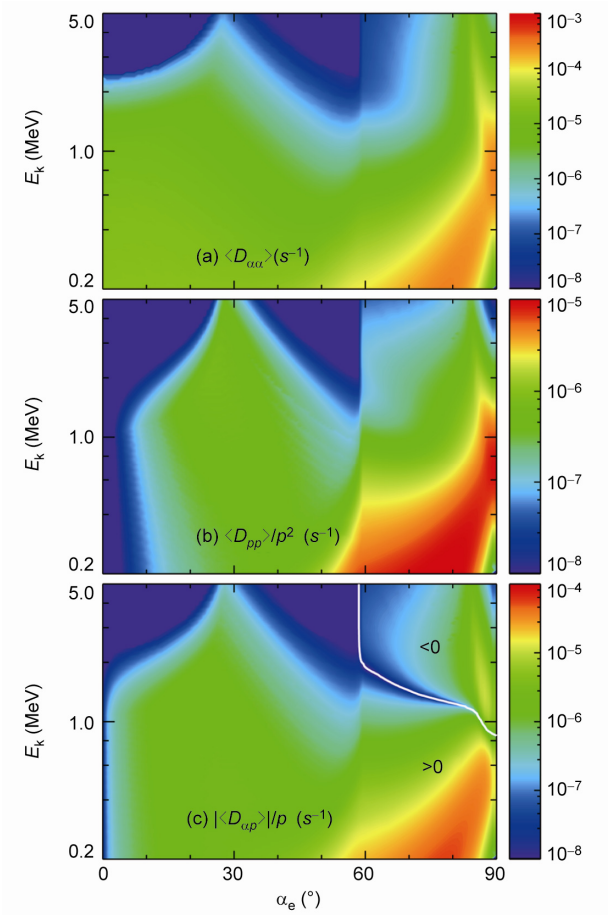

Figure 2 2D bounce-averaged pitch angle (a), momentum (b) and cross (c) diffusion coefficients. Cross term becomes negative above the white line.

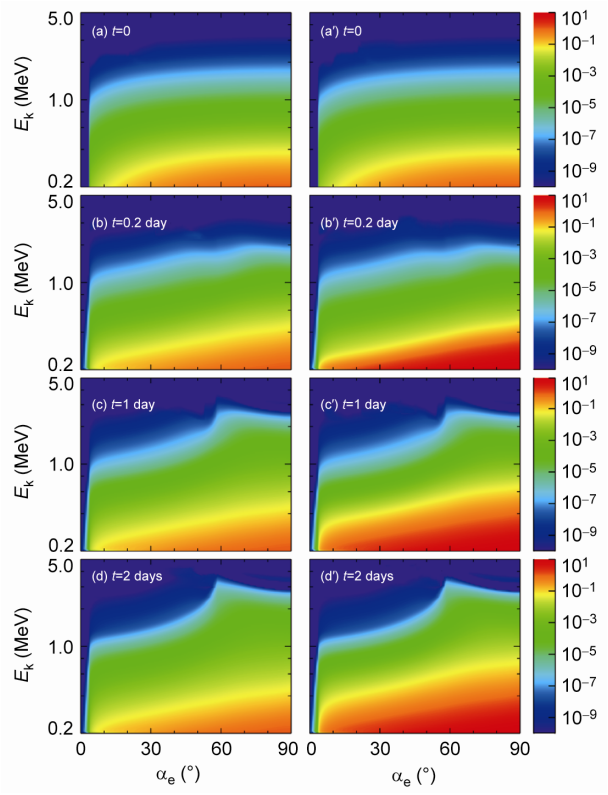

Figure 3 PSD (arbitrary units) at t = 0, 0.2, 1, and 2 days for cases A (left) and B (right). The purple area marks the loss cone.

little influence on the PSD evolution at small pitch angles. Comparison of cases A and B shows that the seed electron injection plays a more important role in the PSD evolution of lower energy electrons.

In Figure 5, we plot PSD ratio of case B (with injection) over case A (without injection) within one day for different energies 0.5, 1.0 and 2.0 MeV. Clearly, the PSD ratio increases as the pitch angle increases, implying that the chorus waves can produce acceleration of the injected seed electrons especially at higher angles and lead to PSD enhancement of the electrons in the radiation belt. In particular, after two days of injection, PSD with injection is found to be a factor of 5–9 higher than that without injection for α_e>60°. Meanwhile, for α_e<40°, PSD with injection is higher than that without injection by a factor of 7 for 0.5 MeV and 1.5 for energies between 1.0 and 2.0 MeV. This is reasonable since the PSD evolution is essentially controlled by the diffusion terms and the diffusion coefficients in the region of α_e>60° and E_k<1.0 MeV are generally one order larger than those coefficients outside this region.

Figure 6 gives variation of electron PSD ratio (B/A) with kinetic energy in the cases of 20°, 70° and 90°. Obviously,

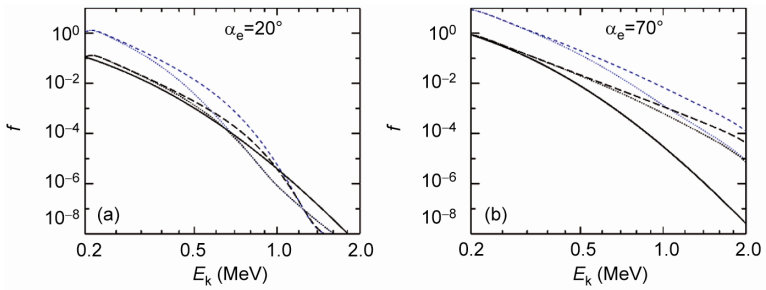

Figure 4 PSD as a function of kinetic energy at fixed equatorial pitch angle with (black) and without (blue) the seed electron injection at times 0 (solid), 1 (dotted) and 2 (dashed) days.

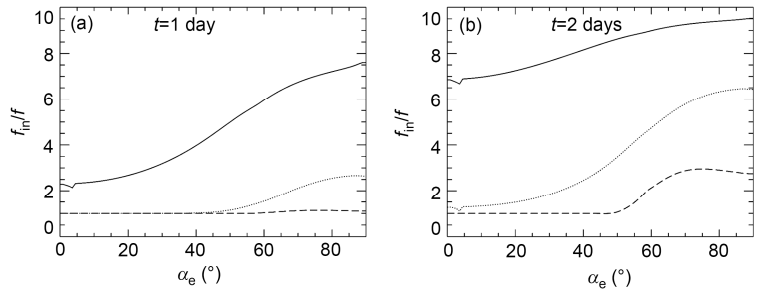

Figure 5 PSD Ratio of tests B to A as a function of equatorial pitch angle in 1 (a) and 2 days (b) for different energies 0.5 (solid), 1.0 (dotted) and 2.0 (dashed) MeV respectively.

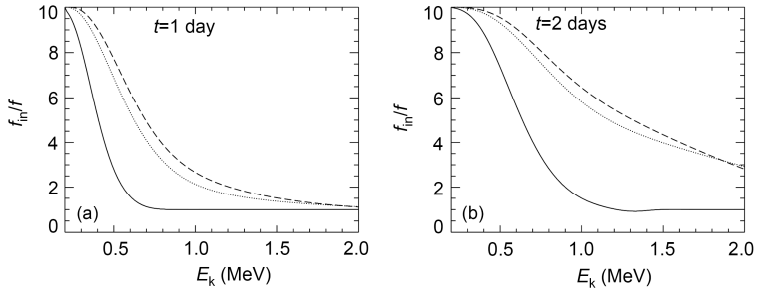

Figure 6 PSD Ratio of tests B to A as a function of kinetic energy in 1 (a) and 2 days (b) for different pitch angles 20º (solid), 70º (dotted) and 90º (dashed) respectively.

the PSD ratio decreases as energy increases since diffusion terms decrease with increasing energy, indicating that enhancement in PSD induced by the seed electrons injection decreases as energy increases. For instance, after two days of injection, PSD with injection is 6 and 3 times of that without seed electron injection for 1 and 2 MeV, respectively.

Here, we focus on the effect of seed electrons with a single energy of 200 keV on the PSD evolution of the radiation belt electrons. We find that seed electron injection affects the lower energy electrons at first and then extends to higher energy electrons. We therefore conclude that the higher the energy is, the shorter the time will be for an obvious PSD variation with energy of MeV.

4 Conclusions

Currently, it has been widely accepted that chorus-driven resonant interaction is an important mechanism responsible for the PSD evolution of electrons in the radiation belt. In this study, we present a quantitative analysis of effect of the seed electron injection on the evolution of the radiation belt electrons via the quasi-linear theory. The obtained results are as follows:

1) When no injection occurs, chorus waves yield acceleration of radiation belt electrons for α_e>60°. For energy below 2.0 MeV, the higher the energy is, the more effective the acceleration is. For energy ranging from 1.0 to 2.0 MeV, electron PSD can increase to 2 or 3 orders of the initial one. However, PSD variation is relatively small at α_e<60°.

2) When injection occurs, chorus waves can efficiently accelerate seed electrons, leading to enhancement in PSD of radiation belt electrons. PSD induced by those seed electrons increases as the pitch angle increases but decreases as energy of electrons increases. Moreover, the PSD evolution can extend to higher energies with a time scale of 1–2 days for energies of 1–2 MeV. Particularly, after two days of injection, PSD can increase to 5–9 times of that without injection at large pitch angles α_e>60°. At small pitch angles α_e<40°, PSD with injection can increase to 7 and 1.5 times of that without injection for 0.5 MeV and 1–2 MeV, respectively. The current result suggests that seed electron injection plays an important role in chorus-driven acceleration of radiation belt electrons. Those features of the PSD evolution are reasonable since the PSD evolution is essentially controlled by the diffusion terms and the diffusion coefficients in the region of α_e>60° and E_k<1.0 MeV are generally one order larger than those coefficients outside this region.

3) In this study, we only consider a simple boundary injection model to simulate the effect of seed electron injection on the PSD of electrons. We assume that seed electrons have a fixed energy of 200 keV and are distributed evenly at the lower boundary energy and pitch angles but only the total number of seed electrons changes. Since seed electron injection is a complicated convection and the energy is not simply fixed, the current injection model is not accurate. However, the current result still provides an influence of the

fixed energy seed electrons on the PSD of radiation belt electrons. More accurate model needs to consider the energy distribution of seed electrons and incorporate the seed electron as a source term into the diffusion equation. Taking into account of the convection features of seed electrons simulation shall become more complicated. Moreover, besides the seed electron injection from the outer boundary, some additional mechanism such as shock compression and ULF modulation can also produce seed electrons and contribute to the PSD evolution of radiation belt electrons [51–53]. We shall leave this in a future study.

This work was supported by the Initiative Project of Chinese Academy of Sciences (Grant No. YYYJ-1110).

1 Lyons L R, Thorne R M, Kennel C F. Pitch-angle diffusion of radiation belt electrons within the plasmasphere. J Geophys Res, 1972, 3: 455–474
2 Paulikas G A, Blake J B. Effects of the solar wind on magnetospheric dynamics-Energetic electrons at the synchronous orbit. Washington DC: American Geophysical Union Geophysical Monograph Series, 1979, 21: 180–202
3 Blake J B, Kolasinski W A, Fillius R W, et al. Injection of electrons and protons with energies of tens of MeV into L less than 3 on 24 March 1991. Geophys Res Lett, 1992, 19: 821–824
4 Reeves G D, McAdams K L, Friedel R H W, et al. Acceleration and loss of relativistic electrons during geomagnetic storms. Geophys Res Lett, 2003, 30: 1529–1533
5 Bortnik J, Thorne R M, O'Brien T P, et al. Observation of two distinct, rapid loss mechanisms during the 20 November 2003 radiation belt dropout event. J Geophys Res, 2006, 111: A12216
6 Su Z P, Xiao F L, Zheng H N, et al. CRRES observation and STEERB simulation of the 9 October 1990 electron radiation belt dropout event. Geophys Res Lett, 2011, 38: L06106
7 Dessler A J, Karplus R. Some effects of diamagnetic ring currents on Van Allen radiation. J Geophys Res, 1961, 66: 2289–2295
8 McIlwain C E. Ring current effects on trapped particles. J Geophys Res, 1966, 71: 3623–3628
9 Kim H J, Chan A A. Fully adiabatic changes in storm time relativistic electron fluxes. J Geophys Res, 1997, 102: 22107–22116
10 Su Z P, Xiao F L, Zheng H N, et al. Combined radial diffusion and adiabatic transport of radiation belt electrons with arbitrary pitch-angles. J Geophys Res, 2010, 115: A10249
11 Su Z P, Xiao F L, Zheng H N, et al. Radiation belt electron dynamics driven by adiabatic transport, radial diffusion, and wave-particle interactions. J Geophys Res, 2011, 116: A4205
12 Baker D N, Blake J B, Klebsadel R W, et al. Highly relativistic electrons in the Earth's outer magnetosphere: 1. Lifetimes and temporal history 1979 – 1984. J Geophys Res, 1986, 91: 4265–4276
13 Schulz M, Eviatar A. Diffusion of equatorial particles in the outer radiation zone. J Geophys Res, 1969, 74: 2182–2192
14 Lyons L R, Thorne R N. Equilibrium structure of radiation belt electrons. J Geophys Res, 1973, 78: 2142–2149
15 Brautigam D H, Albert J M. Radial diffusion analysis of outer radiation belt electrons during the October 9, 1990, magnetic storm. J Geophys Res, 2000, 105: 291–309
16 Horne R B, Thorne R M. Potential waves for relativistic electron scattering and stochastic acceleration during magnetic storms. Geophys Res Lett, 1998, 25: 3011–3014
17 Summers D, Thorne R M, Xiao F L. Relativistic theory of wave-particle resonant diffusion with application to electron acceleration in the magnetosphere. J Geophys Res, 1998, 103: 20487–20500
18 Su Z P, Zheng H N. Simulation of resonant interaction between energetic electrons and whistler-mode chorus in the outer radiation belt. Chinese Phys Lett, 2008, 25: 4493–4496
19 Su Z P, Zheng H N. Resonant scattering of relativistic outer zone electrons by plasmaspheric plume electromagnetic ion cyclotron waves. Chinese Phys Lett, 2009, 26: 129401
20 Thorne R M. Radiation belt dynamics: The importance of wave-particle interactions. Geophys Res Lett, 2010, 37: L22107
21 Su Z P, Zheng H N, Xiong M. Dynamic evolution of outer radiation belt electrons due to whistler-mode chorus. Chinese Phys Lett, 2009, 26: 039401
22 Li W, Shprits Y Y, Thorne R M. Dynamical evolution of energetic outer zone electrons due to wave-particle interactions during storms. J Geophys Res, 2007, 112: A10220
23 Summers D, Ni B B, Meredith N P. Timescales for radiation belt electron acceleration and loss due to resonant wave-particle interactions: 2. Evaluation for VLF chorus, ELF hiss, and electromagnetic ion cyclotron waves. J Geophys Res, 2007, 112: A04207
24 Xiao F L, Zong Q G, Su Z P, et al. Latest progress on interactions between VLF/ELF waves and energetic electrons in the inner magnetosphere. Sci China Earth Sci, 2010, 53: 317–326
25 Xiao F L, Su Z P, Zheng H N. Modeling of outer radiation belt electrons by multidimensional diffusion process. J Geophys Res, 2009, 114: A03201
26 Su Z P, Zheng H N, Chen L X, et al. Numerical simulations of storm-time outer radiation belt dynamics by wave-particle interactions including cross diffusion. J Atmos Sol Phys, 2011, 73: 95–105
27 Su Z P, Zheng H N, Wang S. Dynamic evolution of energetic outer zone electrons due to whistler mode chorus based on a realistic density model. J Geophys Res, 2009, 114: A07201
28 Tsurutani B T, Smith E J. Two types of magnetospheric ELF chorus and their substorm dependences. J Geophys Res, 1977, 82: 5112–5128
29 Burtis W J, Helliwell R A. Magnetospheric chorus—Amplitude and growth rate. J Geophys Res, 1975, 80: 3265–3270
30 Meredith N P, Horne R B, Anderson R R. Substorm dependence of chorus amplitudes: Implications for the acceleration of electrons to relativistic energies. J Geophys Res, 2001, 106: 13165–13178
31 Meredith N P, Horne R B, Thorne R M, et al. Favored regions for chorus driven electron acceleration to relativistic energies in the earth's outer radiation belt. Geophys Res Lett, 2003, 30: 1871–1875
32 Fok M C, Thomas E M, Walther N S. Rapid enhancement of radiation belt electron flux due to substorm depolarization of the geomagnetic field. J Geophys Res, 2001, 106: 3873–3881
33 Kim H J, Chan A A, Wolf R A, et al. Can substorms produce relativistic outer belt electrons? J Geophys Res, 2000, 105: 7721–7735
34 Li X L, Baker D N, Temerin M, et al. Multisatellite observations of the outer zone electron variation during the November 3–4, 1993, magnetic storm. J Geophys Res, 1997, 102: A14123
35 Su Z P, Zheng H N, Xiong M. Dynamic evolution of outer radiation belt electrons due to whistler-mode chorus. Chinese Phys Lett, 2009, 26: 039401
36 Su Z P, Zheng H N, Wang S. A parametric study on the diffuse auroral precipitation by resonant interaction with whistler mode chorus. J Geophys Res, 2010, 115: A05219
37 Su Z P, Zheng H N, Wang S. Three-dimensional simulation of energetic outer zone electron dynamics due to wave-particle interaction and azimuthal advection. J Geophys Res, 2010, 115: A06203
38 Su Z P, Zheng H N, Wang S. Evolution of electron pitch angle distribution due to interactions with whistler mode chorus following substorm injections. J Geophys Res, 2009, 114: A08202
39 Xiao F L, Tian T, Chen L X, et al. Evolution of ring current protons induced by electromagnetic ion cyclotron waves. Chinese Phys Lett, 2009, 26: 119401
40 Xiao F L, Zong Q G, Pu Z Y, et al. Electron acceleration by whistler-mode waves around the magnetic null during 3D reconnection. Plasma Phys. Control Fusion, 2010, 52: 052001, doi: 10.1088/0741-3335/52/5/052001
41 Xiao F L, Su Z P, Zheng H N, et al. Three-dimensional simulations of outer radiation belt electron dynamics including cross diffusion

terms. J Geophys Res, 2010, 115: A05216
42 Xiao F L, Chen L X, He Y H, et al. Modeling for precipitation loss of ring current protons by electromagnetic ion cyclotron waves. J Atoms Slo-Terres Phys, 2011, 73: 106–111
43 Xiao F L, Zhang S, Su Z P, et al. Correlated observations of intensified whistler waves and electron acceleration around the geostationary orbit. Plasma Phys. Control Fusion, 2012, 54: 035004, doi: 10.1088/0741-3335/54/3/035004
44 Xiao F L, Zhang S, Su Z P, et al. Rapid acceleration of radiation belt energetic electrons by Z-mode waves. Geophys Res Lett, 2012, 39: L03103
45 Su Z P, Xiao F L, Zheng H N, et al. STEERB: A three-dimensional code for storm-time evolution of electron radiation belt. J Geophys Res, 2010, 115: A09208
46 Kozyra J U, Rasmussen C E, Miller R H, et al. Interaction of ring current and radiation belt protons with ducted plasmaspheric hiss. 1: Diffusion coefficients and timescales. J Geophys Res, 1994, 99: 4069–4084
47 Glauert S A, Horne R B. Calculation of pitch angle and energy diffusion coefficients with the PADIE code. J Geophys Res, 2005, 110: A04206
48 Summers D. Quasi-linear diffusion coefficients for field-aligned electromagnetic waves with applications to the magnetosphere. J Geophys Res, 2005, 110: A08213
49 Albert J M, Young S. Multidimensional quasi-linear diffusion of radiation belt electrons. Geophys Res Lett, 2005, 32: L14110
50 Xiao F L. Modelling energetic particles by a relativistic kappa-loss-cone distribution function in plasmas. Plas Phys Contl Fusion, 2006, 48: 203–207
51 Zong Q G, Zhou X Z, Li X, et al. Ultralow frequency modulation of energetic particles in the dayside magnetosphere. Geophys Res Lett, 2007, 34: L12105
52 Zong Q G, Wang Y F, Yiang B, et al. Recent progress on ULF wave and its interactions with energetic particles in the inner magnetosphere. Sci China Ser E-Tech Sci, 2008, 51: 1620–1625
53 Zong Q G, Zhou X Z, Wang Y F, et al. Energetic electron response to ULF wave induced by interplanetary shocks in the outer radiation belt. J Geophys Res, 2009, 114: A10204, doi: 10. 1029/2009JA014-393